EXPERIMENTAL STUDIES OF LONGITUDINAL DYNAMICS OF SPACE-CHARGE DOMINATED ELECTRON BEAMS*

D. X. Wang†, Institute for Plasma Research, University of Maryland, College Park, Maryland 20742

A comprehensive experimental program was carried out at the University of Maryland Beam Transport facility to study the longitudinal beam physics of space-charge dominated bunches. This investigation included the behavior of (a) bunches with parabolic line charge profile, (b) bunches with rectangular line charge profile, and (c) local perturbations (slow and fast waves) in rectangular bunches. The major experimental results are presented in this paper.

I. INTRODUCTION

High-intensity charged particle beams have many applications such as high energy linear accelerators, radioactive waste burners, induction linacs as Heavy Ion Inertial Fusion (HIF) drivers, free electron lasers (FEL), and high power microwave generators. In many cases high beam current and power are desired, and the beam dynamics is in a space-charge dominated regime. The appearance of the strong space-charge force complicates the beam dynamics, may degrade the beam quality and limit applications. The objective of this project was to understand the longitudinal beam physics of space-charge dominated beams.

The space-charge force is a collective effect due to the repulsive coulomb interaction between particles. It is a function of the space-charge distribution and the boundary conditions and is always defocusing. The space-charge force is often nonlinear and time-dependent. In general, beam dynamics becomes space-charge dominated if the beam size is primarily determined by the space-charge, instead of the emittance. This condition usually occurs at relatively high beam current and non relativistic energies. For coasting beams this means that the space-charge wave velocity is much larger than the velocity spread, i.e. $c_s >> \Delta v$, (more than 30 times larger in our experiments) where the wave velocity is $c_s = \sqrt{egI/4\pi e_0 mv\gamma^5}$, I is the beam current, v is the beam velocity, and g is a geometry factor that will be discussed later. The longitudinal space-charge field which can be expressed analytically as [1]

$$E_Z(z,s) = -\frac{g}{4\pi\varepsilon_0\gamma^2}\frac{\partial\Lambda(z,s)}{\partial z}, \qquad (1)$$

where Λ is the line charge density, z is the longitudinal coordinate in the beam frame, and s is the travel distance. Equation (1) was derived for a coasting beam under long wavelength approximation and is widely used for bunched beams where the bunch length 2Z is much longer than the beam diameter 2a. The geometry factor g is an important parameter in longitudinal dynamics that is introduced by the boundary conditions and represents the transverse and longitudinal coupling. The g factor is treated as a constant in Eq. (1) though in practice it is a variable of time since the beam radius varies in time and along the bunch. Generally, the space-charge field can be obtained by solving Maxwell's equations numerically for a given boundary and charge distribution.

Our experiments were chosen to explore the beam behaviors in different dynamic regimes. The first series of experiments were conducted to study linear behavior with a parabolic line charge profile having a linear space-charge force given by Eq. (1) [2, 3]. The second series of experiments were performed with a rectangular bunch (uniform line charge density) to investigate the nonlinear behavior since there is little space-charge force at the flat region but very strong force on the ends that causes rapid edge expansions [4]. Finally, space-charge wave experiments were carried out to study the linear wave behavior on a "coasting" beam, i.e. fast and slow waves as propagation of localized velocity and density perturbations [5, 6, 7].

The experimental configuration will be briefly described first. Then three series of experiments will be discussed separately with brief introductions of theoretical models, and important experimental results are presented. At the end, a short summary is given.

II. EXPERIMENTAL CONFIGURATION

The experiments were performed at the University of Maryland Electron Beam Transport facility consisting of a short-pulse electron beam injector, a 5-meter periodic solenoid-focusing transport channel, and an upgraded diagnostic system [8]. A schematic drawing of the experimental setup is shown in Fig. 1. The key components included a gridded electron gun that can produce parabolic beams and localized perturbations on beams and can vary the beam energy and current by adjusting operating parameters; five fast wall-current monitors with 1.2 GHz bandwidth and three time-resolved energy analyzers, installed along the channel; a compact induction module producing a quadratic time-dependent accelerating voltage.

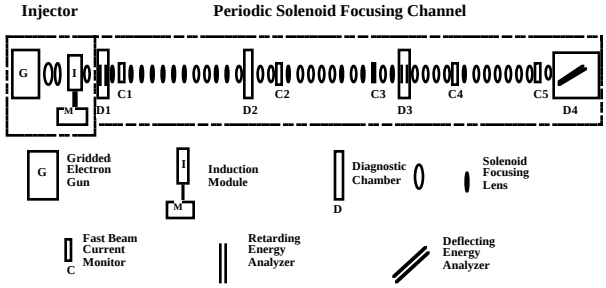

Fig. 1. Schematic of experimental setup.

Typical beam parameters were a few keV in beam energy, a few tens of mA in current, a few tens of ns in pulse duration, about 5 mm in beam radius, and beam pipe radius of 19 mm.

* Supported by Department Of Energy

† Present address: CEBAF, Newport News, VA 23606

III. PARABOLIC BUNCH EXPERIMENT

The longitudinal dynamics of a parabolic bunch can be described by a longitudinal envelope equation [9. 10], written as

$$\frac{d^2Z}{ds^2}-\frac{2gZ_iI_p(0)}{\beta_0^3I_0}\frac{1}{Z^2}-\frac{\varepsilon_L^2}{Z^3}=0, \qquad (2)$$

where 2Z is the full longitudinal bunch length, $2Z_i$ is the initial bunch length, $I_0=4\pi\varepsilon_0 m_e c^3/e=17\text{kA}$ for electrons, I_p is the peak current, and ε_L is the longitudinal emittance of the beam. If the beam is space-charge dominated, the third term in Eq. (2) is negligible comparing to the second term. On the other hand, this condition defines a space-charge dominated beam for parabolic bunches. Then an analytical solution can be readily found by integrating Eq. (2) twice [3]. According to this 1-D envelope model the parabolic shape is preserved and the velocity distribution remains linear. The bunch length, or the peak current and the slope of the velocity distribution are determined by Eq. (2).

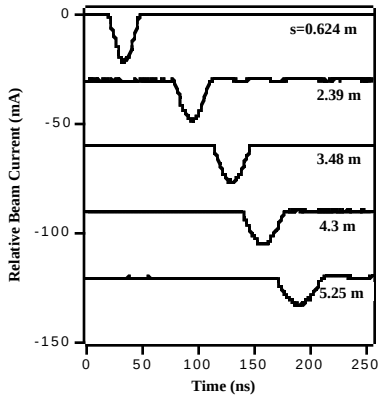

Fig. 2. Beam current signals of a parabolic bunch at different locations along the channel without a velocity tilt.

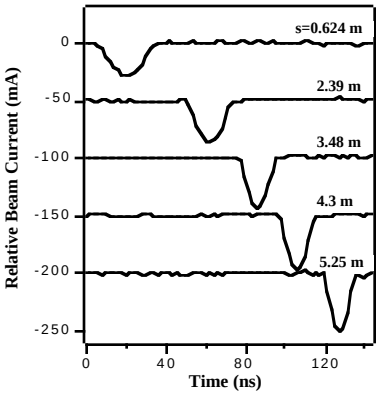

Fig. 3. Beam current signals of parabolic bunch with an initial tilt Z'=-0.092.

In the experiment, a parabolic beam with a constant velocity was produced and launched into the channel. Current profiles of a drift parabolic bunch, measured at different channel locations, is shown in Fig. 2. Also the parabolic beams were compressed by the induction accelerating voltages with various slopes. A typical case is shown in Fig. 3. For each case, the bunch lengths were obtained by fitting the current profiles with the parabolic curves, and are plotted in Fig. 4 in comparison with the results from the envelope equation where a constant g was used. The experiment and theory were in very good agreement. To verify the transverse dependence of the g factor, the focusing strength was varied, giving different beam radius, and the result is plotted in Fig. 5. The velocity distribution was also measured and plotted in Fig. 6 for a drift expanding beam, showing the linearity predicted by the theory. In the experiment, it was observed that the longitudinal envelope was insensitive to the transverse mismatching oscillations, which was later confirmed by a 2-D simulation of particle code [11].

IV. RECTANGULAR BUNCH EXPERIMENT

For rectangular beams, i.e. a uniform line charge density, the longitudinal space-charge force is highly nonlinear, with little force at the flat region but very strong forces at the ends [12, 13]. In general, the 1-D cold fluid model can be employed to describe the longitudinal beam dynamics. The fluid equations can be written as

$$\begin{aligned}&\frac{\partial\Lambda}{\partial t}+v\frac{\partial\Lambda}{\partial z}+\Lambda\frac{\partial v}{\partial z}=0\\&\frac{\partial v}{\partial t}+v\frac{\partial v}{\partial z}\approx\frac{e}{m\gamma^3}E_z=-\frac{eg}{4\pi\varepsilon_0 m\gamma^5}\frac{\partial\Lambda}{\partial z}\end{aligned} \qquad (3)$$

where Λ is the line charge density and v is the particle velocity in the beam frame. Analytic solutions can be obtained by the method of characteristics in the practically interested regime. One of the important properties of the fluid equations is the time-reversibility, i.e. Eqs (3) are invariant by changing the sign of t (therefore, changing the sign of v as well).

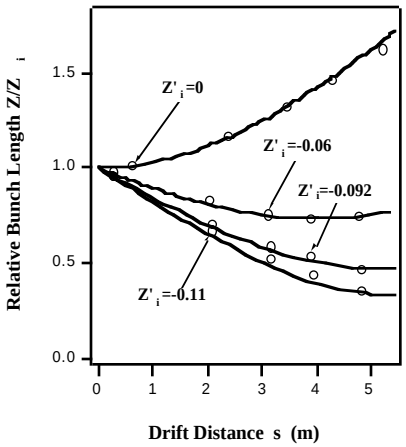

Fig. 4. Normalized bunch length vs. drift distance for parabolic beams with different initial tilts, where the circles represent experiment while the solid curves are from envelope calculation.

For an initial rectangular beam with a constant velocity, the beam edge erodes towards the beam center at a speed of c_s and expands towards vacuum at $2c_s$, due to the strong space-charge force at the ends. The density profile is quadratic and the velocity distribution is linear at the ends, while the center region remains non-perturbed. There is a "cusp" point where the edge erosions reach the

beam center and the velocity distribution becomes linear along the entire bunch . Utilizing the time reversibility the initial rectangular bunch shape can be reconstructed by imparting an appropriate linear velocity tilt at the "cusp" location, which changes the sign of the velocity in the beam frame. The detailed description and a schematic of this process can be found in Ref. [3].

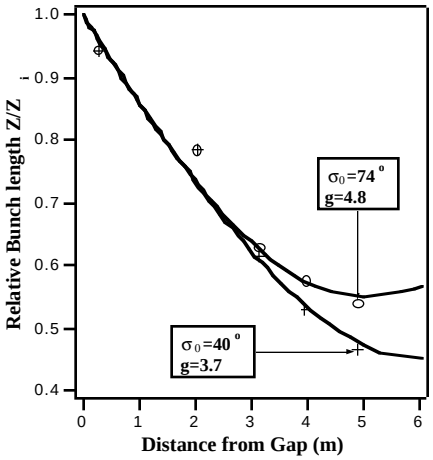

Fig. 5. Normalized bunch length vs. drift distance for different focusing strengths where the circles and the crosses represent experiment while the solid curves are from calculations.

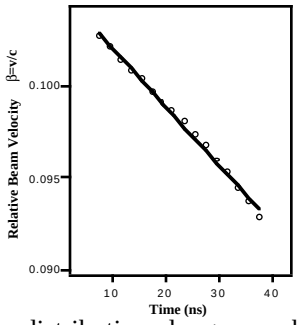

Fig. 6. Velocity distribution along a parabolic bunch after certain distance of the drift expansion, where the circles represent experiment while the solid line for linear fit.

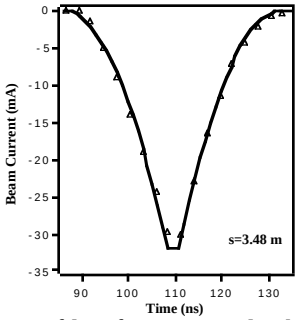

Fig. 7. Current profile of a rectangular bunch just before the cusp point, after certain drift distance.

In the reconstruction experiment, we first demonstrated the linear velocity distribution at the "cusp" point by adjusting the bunch length so that the "cusp" point appeared at the second energy analyzer. Figure 7 shows the current profiles of an expanding rectangular bunch just before the cusp point. The velocity distribution was also measured and is shown in Fig. 8, which was very linear as predicted by the theory. The measurement result (circles), simulation (triangles), and calculations (solid line) were in very good agreement. Here beam energy, current and pulse duration were 2.5 keV, 35 mA, and 17.5 ns, respectively. In the experiment the pulse duration was carefully adjusted to let the cusp point happen at the second energy analyzer.

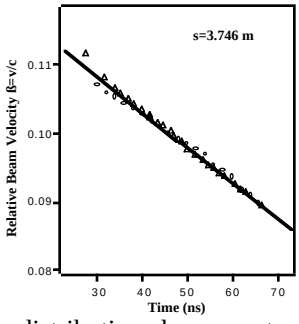

Fig. 8. Velocity distribution along a rectangular bunch after certain distance of drift expansion, where circles represent experiment while solid curve theory.

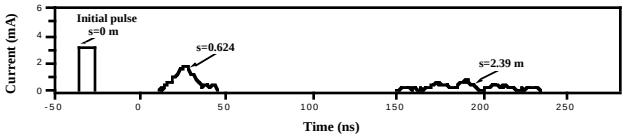

Fig. 9a. Current profiles for a short drift rectangular bunch without induction acceleration voltage.

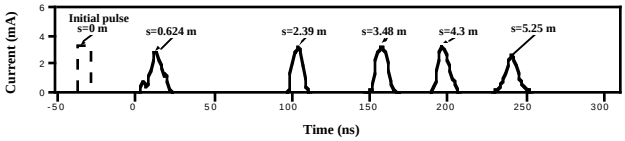

Fig. 9b. Current profiles along channel for a short drift rectangular bunch with an appropriate velocity tilt imparted by induction module.

Due to the short distance (0.34 m) between the gun and induction module where a linear velocity tilt was imposed, a 300 eV, 3.3 mA. and 7 ns beam was used to increase the wave velocity and slow down the traveling speed. Without application of the induction acceleration and velocity tilt the beam expanded rapidly and disappeared at the third current monitor, shown in Fig. 9a. The bunch length at the second current monitor was consistent with the calculation, though the noise became substantial due to the very low beam current. With a proper induction acceleration to impart the linear velocity tilt, the bunch shape was reconstructed, shown in Fig. 9b. The distinguishing features of the reconstruction process were that the peak current in the flat region remained the same, the leading and falling edges became steep, and the flat top maintained a constant velocity. In the experiment we also varied the beam pulse duration, the slopes of the velocity tilt, and the beam center energy after the induction module. In each case the beam behaved consistently with the theory. Due to the low beam current, the measurement of constant velocity distribution predicted at the reconstruction point was not available.

It is noted that the time reversibility is a general property of the fluid equations. Therefore, in principle, the

reconstruction process can be performed any where as long as the appropriate velocity distribution was generated. In practice, however, it is easiest to generate a linear ramp of acceleration.

V. SPACE-CHARGE WAVE EXPERIMENTS

The initial localized perturbations were introduced to the beam by creating small positive voltage bumps on the cathode-grid pulse, which generated both initial localized velocity and density perturbations. These initial perturbations propagated as space-charge waves, i.e. fast and slow waves moving forward and backward in the beam frame, respectively. In the experiment, we generated not only a pair of fast and slow waves, shown in Fig. 10, but also single fast and single slow waves. An analytical solution was found to interpret the experimental observations [5]. Figure 11 shows the current signals of the space-charge waves from the energy analyzer. The signals represented the perturbed electrons with an energy above the average beam energy, where the left bump corresponded to the fast wave and the right to the slow wave. The fast and slow waves had separated after a drift distance. In obtaining this set of traces, the only difference was change of the gun operating condition that determined the different initial perturbations of the velocity and the density. In general two space-charge waves in the form of localized perturbations were generated with different amplitudes in the velocity and the density, depending on the initial conditions.

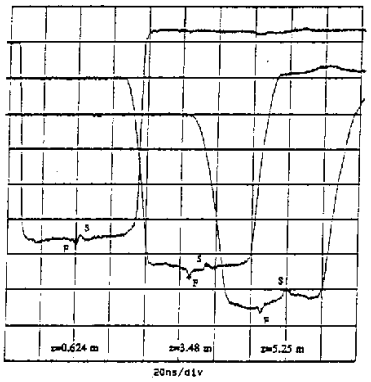

Fig. 10. Current profiles along channel with initial perturbation propagating as fast and slow waves.

The localized fast and slow waves propagated away from each other at speed of c_s in the beam frame. By measuring the time interval between the two waves and the traveling distance of the beam, the wave velocity can be determined by a linear fitting, shown in Fig. 12 and calculated from a formula $\Delta t=2c_s s/(v_0^2-c_s^2)$, where Δt was the time interval between the fast and slow waves, s was the drift distance, and v_0 was the beam velocity. From the measured wave velocity, the geometry factor can be found according to the relation between c_s and g given above. An average beam radius was measured using a movable florescent screen and a CCD camera, shown in Fig. 13. The measured radius was in a very good agreement with calculation under smooth approximations [14]. The result showed that g=2lnb/a, where b was the pipe radius and a was the average beam radius, which was consistent with the theory under the assumption of a constant volume charge density [1]. This also implies that the space-charge field is a constant across the transverse cross section.

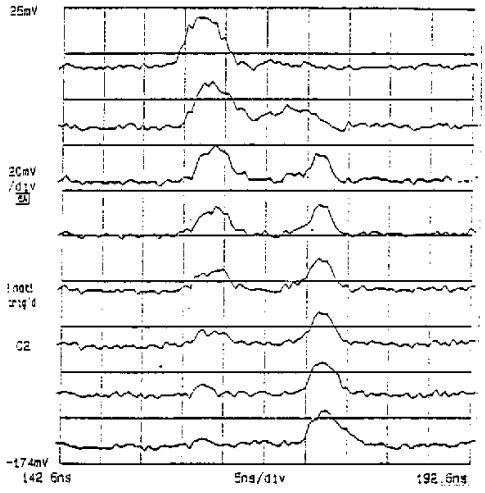

Fig. 11. Current signals are perturbed electrons at one of the retarding energy analyzers. Initial perturbation becomes two waves, fast and slow, after certain drift distance.

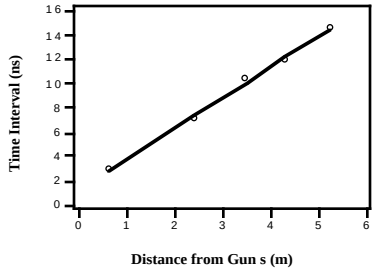

Fig. 12. Time intervals between fast and slow waves vs. drift distance, where the circles represent experiment and the solid line is linear fit.

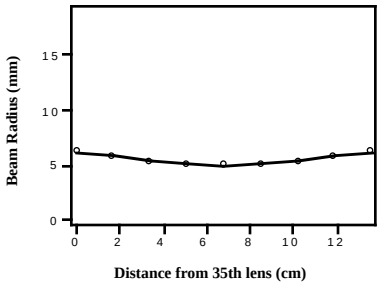

Fig. 13. Measured beam radius vs. longitudinal distance.

The experiments were also conducted to investigate the wave behaviors at ends of the rectangular bunch, where the ends were referred to as the boundary between the flat region and the finite edge. The initial perturbation was moved to very close to the beam end. The slow wave hit the eroding end shortly and split into reflected and transmitted waves, shown in Fig. 11. The reflected slow wave became a fast wave moving forward. Due to the edge expansion and erosion, the reflected wave and the edge moved forward at the same wave speed. The transmitted wave could not reach the zero density point because the zero density point kept moving out at twice of the wave speed. Figure 12 plots the time interval between the fast

wave and the reflected wave and the fast and the transmitted waves. The wave velocity of the reflected wave changed as approaching the beam end and became c_S afterwards while the transmitted wave remained at a constant wave velocity c_S. In the experiment, a single fast wave with rather large amplitude was launched close to the bunch front end, and the clear reflection and transmission were seen [15]. It was also qualitatively observed that the steeper the edge, the stronger the reflection.

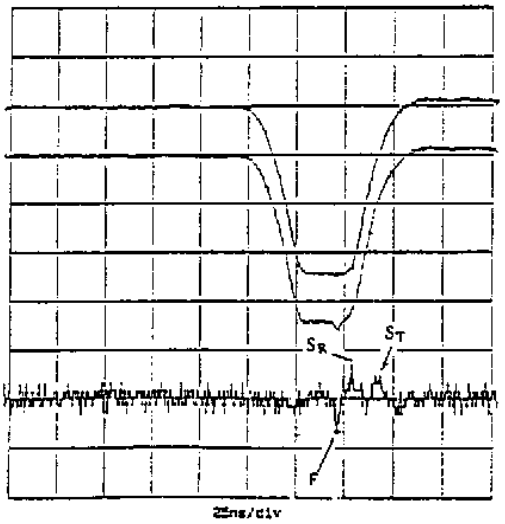

Fig. 14. Current profiles after certain drift distance with and without perturbation (top two traces, respectively), showing the original fast wave (F), the reflected slow wave (S_R), and the transmitted slow wave (S_T), while the bottom trace is the difference of the two top traces.

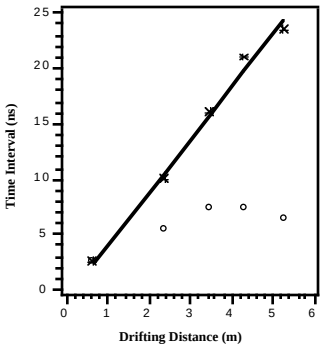

Fig. 15. Time separations between the original fast wave and the transmitted slow wave (stars), and between the original fast wave and the reflected slow wave (circles), vs. drift distance.

VI. CONCLUSION

The self-consistent parabolic profile and linear velocity distribution were experimentally verified. The experimental results were in very good agreement with the envelope model. The linear velocity distribution at the cusp point, predicted by the fluid model was experimentally obtained for a drift rectangular bunch. The pulse reconstruction of rectangular bunch, based on the time-reversibility was experimentally demonstrated. Both single fast and single slow space-charge waves were generated in the experiment. In general, a pair of fast and slow waves was generated with different amplitudes, depending on the initial perturbation conditions. The geometry factor was experimentally determined for space-charge dominated coasting beams, which was consistent with the theory under assumption of a constant volume density, rather than a constant radius for the emittance dominated beams. The reflection and transmission of the waves at the beam ends were observed in the experiment.

Overall, 1-D models worked surprisingly well. A constant g factor was a good approximation for both parabolic and rectangular beams. The longitudinal dynamics was insensitive to transverse mismatch oscillations.

VII. ACKNOWLEDGMENT

The author would like to express deepest gratitude to his dissertation adviser, Prof. M. Reiser and co-adviser Dr. J. G. Wang for their guidance. He thanks the former colleagues at Maryland, in particular Dr. D. Kehne and H. Suk for their contributions to this project and Dr. I. Haber of NRL for permitting the use of his SHIFTZ code and many fruitful discussions. The author would also like to acknowledge the Division of High Energy Physics and the Division of Advanced Physics and Technology of DOE for their support.

VIII. REFERENCES

[1] M. Reiser: Theory and Design of Charged Particle Beams, Wiley & Sons, New York.

[2] J. G. Wang, D. X. Wang, and M. Reiser, Appl. Phys. Lett., **62**(6), pp. 645-647, 8 Feb. 1993.

[3] D. X. Wang, J. G. Wang, D. Kehne, and M. Reiser, Appl. Phys. Lett., **62**(25), pp. 3232-3234, 21 June 1993.

[4] D. X. Wang, J. G. Wang, and M. Reiser, Phys. Rev. Lett. **73**(1), pp. 66-69, July 4, 1994.

[5] J. G. Wang, D. X. Wang, and M. Reiser, Phys. Rev. Lett., **71**(12), pp. 1836-1839, September 20, 1993.

[6] J. G. Wang, H. Suk, D. X. Wang, and M. Reiser, Phys. Rev. Lett., **72**(13), pp. 2029-2032, March 28, 1994.

[7] J. G. Wang, D. X. Wang, H. Suk, and M. Reiser, Phys. Rev. Lett., **74**(16), pp. 3153, April 17, 1995.

[8] J. G. Wang, D. X. Wang, and M. Reiser, Nucl. Instr. & Meth. in Phys. Res. A 316, pp. 112-122, 1992.

[9] L. Smith, "ERDA summer study for heavy ion inertial fusion" (ed. R. O. Bangerter, W. B. Herrmannsfeldt, D. L. Judd, and L. Smith), LBL-5543 (1976), pp. 77-79.

[10] D. Neuffer, IEEE Trans. on Nuclear Science, **26**(3), pp. 3031-3033, June 1979.

[11] A. Faltens, E.P. Lee, and S.S. Rosenblum, J. Appl. Phys., **61**(12), 5219 (1987).

[12] I. Haber, private communications.

[13] D.D. Ho, S.T. Brandon, and E. P. Lee, Particle Accelerator, Vol. **35**, 15 (1991).

[14] H. Suk, M. Reiser, J. G. Wang, and D. X. Wang, Appl. Phys. Lett., **76**(7), pp. 3970-3974, 1 October 1994.

[15] J. G. Wang and M. Reiser, in these proceedings.